ELSEVIER

Physica D 76 (1994) 359–368

PHYSICA D

Vulnerability in excitable Belousov–Zhabotinsky medium: from 1D to 2D

M. Gómez-Gesteira, G. Fernández-García, A.P. Muñuzuri, V. Pérez-Muñuzuri, V.I. Krinsky[1], C.F. Starmer[2], V. Pérez-Villar

Group of Nonlinear Physics, Facultade de Física, Universidade de Santiago de Compostela, 15706 Santiago de Compostela, Spain

Received 26 May 1993; revised 1 February 1994; accepted 3 February 1994
Communicated by A.V. Holden

Abstract

Mechanisms for initiating rotating waves in 1D and 2D excitable media were compared and parameters affecting wavefront formation were analyzed. The time delay between two sequentially initiated wavefronts (a conditioning wave followed by a test wave) was varied in order to induce rotating waves, a protocol similar to that utilized in cardiac muscle experiments to reveal *vulnerability* to rotating wave initiation.

We define the vulnerability region, VR, as the range of time delays between conditioning and test waves where the test waves evolves into a rotating wave. The smaller the VR, the more resistant the heart is against origination of dangerous cardiac arrhythmias. Heterogeneity of cardiac muscle is widely recognized as the prerequisite for rotating wave initiation. We have identified the VR in homogeneous 2D excitable media. In the Belousov–Zhabotinsky (BZ) reaction with immobilized catalyst and in the Oregonator model of this reaction, a properly timed test wave gives rise to rotating waves. The VR was increased when the size of the perturbation used for test wave creation was increased or when the threshold for propagation was decreased. Increasing the dimensionality of the medium for 1D to 2D results in diminishing of VR.

1. Introduction

During the last two decades different approaches have been used to explain the appearance and existence of spiral waves [1–5]. Phenomena relative to the excitation and re-excitation of a medium have attracted for years the interest of scientists in different fields. Heart muscle [6], retina [7] and cultures of the slime mould *Dyctiostelium Discoideum* [8] constitute classical examples of spiral appearance in excitable media. While the importance of spiral waves in some of these preparations is unclear, in cardiac tissue, spiral waves reflect self-maintained activation that can degenerate into potentially life-threatening arrhythmias.

Vulnerability of cardiac muscle to initiation of reentrant arrhythmias is usually experimentally

[1] Present address: Institut Non-Lineaire de Nice, 06560 Valbonne, France.

[2] Current address: Duke University Medical Center, Durham, North Carolina 27710, USA and Division of Biomedical Engineering, India Institute of Technology, Madras, India 600 036.

SSDI 0167-2789(94)00024-K

determined using the following stimulation protocol. Two sequential electric pulses (conditioning and test) are delivered to the cardiac preparation and the parameter region (time delay, stimulus amplitude, etc.) where rotating waves are created is measured. In these experiments three classes of responses are typically found. (1) When the interval between conditioning and test pulses is much longer than the restoration time (called *refractoriness* in cardiology) both pulses initiate wavefronts that propagate in all directions (we will call this a class 1 response). (2) When the interval between the pulses is shorter than the restoration time, only the first pulse initiates a propagating response (we will call this a class 2 response). (3) When the interval between the pulses is slightly larger (several percent) than the restoration time, the test pulses elicit a train of responses (we will call this a class 3 responses). Initiating a train of responses by properly timed stimuli is called *vulnerability* and the range of delays between the conditioning and the test wave is called the *vulnerable region* (VR). The larger the VR, the less resistant the cardiac muscle to cardiac arrhythmias initiation.

Initiation of these rhythms by specific stimulation protocols was well known within the area of cardiac electrophysiology. However, only recently have the detailed mechanisms for initiation been studied. Allessie et al. [6] demonstrated the initiation of rotating waves in cardiac tissue by means of vulnerability experiments. However, the determinants of the VR have not been characterized, in spite of the variety of approaches carried out during the last decade [9–12].

Keener and Phelps [13] described numerically this mechanism for the FitzHugh–Nagumo and Beeler–Reuter models. They came to the conclusion that vulnerability was a characteristic of a discrete anisotropic cellular medium where the wave fails to propagate in one direction (weak coupling), leading to a permanently rotating wave. In their model for a continuous medium, the response either fails to propagate in al directions or propagates in all directions, i.e there is no possibility for spiral wave initiation.

We have found a vulnerable region similar t that described in cardiology in a 2D continuou Belousov–Zhabotinsky (BZ) [14] reaction, an have explored the parameters that control th VR. We have found both numerically and ex perimentally that the VR can be reduced b increasing the excitability of the system or b increasing the dimensionality of the medium.

2. Experimental setup

The experiments were performed in a B medium, where the catalyst (ferroin 0.008 M was immobilized in a silica gel [15]. The gel wa 1 mm thick in a Petri dish of 6.1 cm in diamete The petri dish was filled with the followin recipe: 1/6 M $CH_2(COOH)_2$, 1/6 M NaBrO and various H_2SO_4 concentrations to get diffe ent excitabilites [16] in the system. The depth o the liquid layer was greater than 5 mm to prevei any interference between the oxygen in the a and the BZ reaction. The experiments wei performed at room temperature (25 ± 1°C).

Once a wave (*conditioning* wave) passed given point by a known distance, the mediu was stimulated at the point by touching the g with a silver wire [17] (0.3 mm in diameter), fo a period of 5 seconds. Due to the uncertainty the position of the stimulus (a result of the fini thickness of the silver wire), the experimen were performed several times under the sam conditions in order to achieve an adequa statistical sample.

All the experiments were followed with CCD camera and recorded on a videotap Digital image processing was carried out.

Similar experiments have been carried o using a liquid system [18]. A gel system presen several advantages that permit the study of the phenomena with high accuracy. In the gel sy tem, the interaction between oxygen and the B

reaction is avoided, as the gel is covered by a liquid layer and the mechanical disturbances created by the electrode in the liquid layer do not affect the waves appearing in the reaction. In addition, convection is also avoided. Only in the gel system can *quasi two-dimensional* pulses be generated (as silver wire only touches the upper surface of the gel).

Thus, it is possible to separate 2D from 3D effects. By varying the thickness of the gel it is possible to study the transitions from 2D to 3D [19].

3. Model

Simulations were performed with the two-variable version of the Oregonator model [20] using Tyson's "Lo" parameters [21]. The equations for a two-dimensional medium are:

$$\frac{\partial u}{\partial t} = \frac{1}{\varepsilon}\left(u - u^2 - fv\frac{(u-q)}{(u+q)}\right) + D_u \Delta u\,,$$
$$\frac{\partial v}{\partial t} = u - v\,, \qquad (1)$$

where u is the *propagator* variable representing the dimensionless concentration, $[HBrO_2]$, and v, the *recovery* variable, is the dimensionless concentration [ferriin]. f, q and ε are parameters determined by the kinetics of the BZ reaction.

The diffusion coefficient of the recovery variable was considered to be zero to mimic the propagation of waves in a silica gel, where the ferroin was immobilized.

All simulations were performed with $q = 0.002$ and $f = 3.0$, in such a way that the nullclines intersected at a single point. This point was placed in the stable branch, which constitutes an excitable system.

Both in the 1D and in the 2D studies, the mesh size and the time step were considered to be 0.16 and 10^{-3} respectively, and the system rescaled to have a diffusion coefficient $D_u = 1$.

The set of equations (1) was solved by using an Euler method, where the Laplacian operator was discretized by means of finite differences (using two neighbours in 1D and four in 2D). Von Neuman boundary conditions were used in both calculations.

The technique used to simulate the experimental mechanism was as follows: the control point (p_c) was placed at a given grid point. When the maximum of a wave arrived at that position, time was reset to zero and a given time delay (t_d) was fixed by the computer before introducing a perturbation in the u variable. This perturbation was established at p_c and at its closest neighbours (5 grid points in 1D and 5×5 in 2D). In general, the amplitude of the perturbation was fixed to the maximum value of u in the wave. Several behaviours, depending on the value of t_d, were observed as explained in the following section.

4. Results

The three classes of responses described in the introduction were observed in experiments with the BZ reaction. We observed that a pulse delivered after a conditioning wave with a delay larger than the refractoriness (restoration) period propagated in all directions; for short delays, no response was observed; and for intermediate delays, a wavefront propagated in some directions and failed in others (broken wavefront).

This phenomenon is illustrated in Fig. 1. In Fig. 1a, a conditioning wave and responses to two test stimuli ($s1, s2$) delivered at different distances (different time delays) from the conditioning wave are shown.

The $s1$ response evolved into a circular wave, while the $s2$ response evolved into a pair of spirals (Fig. 1b). The same behaviour is shown in figs. 1c,d for the Oregonator model.

When the numerical approach was carried out in a 1D excitable medium (analog to a nerve or cardiac fiber), the three classes of responses previously mentioned were obtained once again. (1) Delays larger than the refractoriness period resulted in wavefronts propagating away from

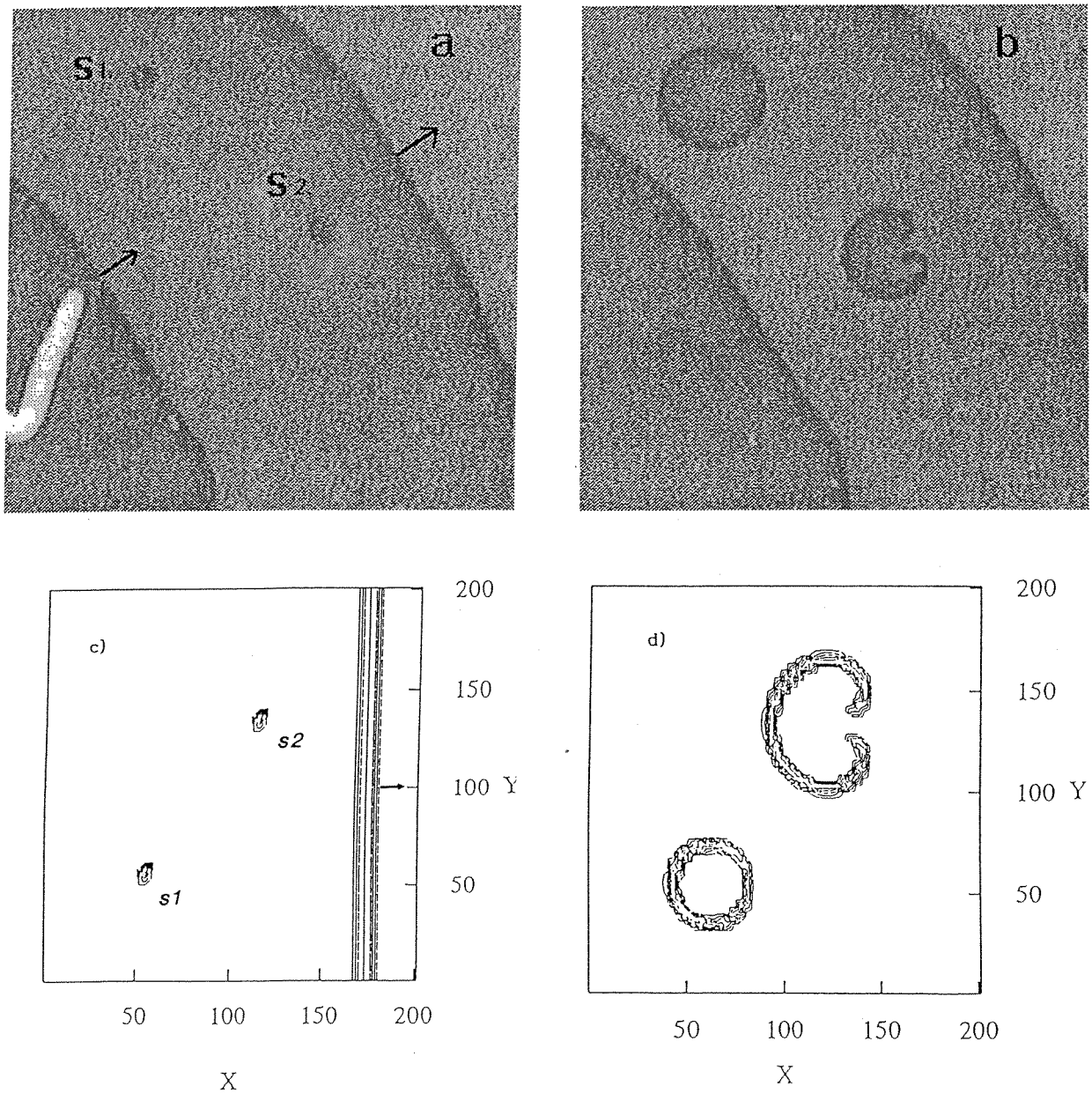

Fig. 1. Vulnerability in 2D. (a) Two stimuli were delivered to the BZ reaction (dark points marked $s1$ and $s2$) by touching it with a silver electrode (seen at the left). The arrow shows the direction of propagation of the conditioning wave, CW. Stimulus $s1$ was delivered 190 seconds after CW passage through that point, and stimulus $s2$ 160 seconds after CW. (b) Image taken 285 seconds later than (a). Stimulus $s1$ gave rise to a circular wave and stimulus $s2$ to two spirals. Initiation of spirals corresponds to the vulnerability phenomenon in cardiac muscle. (The recipe is given in the text, here H_2SO_4 was 1/12 M). (c), (d) The same behaviour in the Oregonator model (parameters $f = 3.0$, $\varepsilon = 0.05$, $q = 0.002$).

the stimulation site in both directions. This is qualitatively similar to 2D – in 2D a circular wave was initiated, while in 1D the result is two pulses propagating in opposite directions. (2) For short delays no response was observed (exactly the same as in a 2D medium). (3) For intermediate delays, the result was a wave propagating away from the stimulation site in the direction opposite to the conditioning wavefront (similarly to 2D, where propagation failed in some directions, resulting in a discontinuous wavefront).

This is shown in Fig. 2. In panel (a), the time delay for delivering the test pulse ($s1$) is large, and the response propagates in all directions. In panel (b), the time delay is short enough and the test response propagates only in the direction opposite to the conditioning wavefront.

The most interesting difference between 1D and 2D was the evolution of different patterns of propagated responses we observed when a parameter (the time delay) was progressively increased. In 1D, the transition from no propagation (class 2 described in the introduction) to unidirectional propagation (class 3) and then, to bidirectional propagation (class 1) was observed and each class of response was invariant with respect to time since wavefront initiation.

We expected that in the 2D medium, a similar, time-invariant, sequence of patterns would be observed as the time delay was increased: no propagation (class 2) followed by discontinuous propagation (class 3) and then propagation of a continuous wavefront (class 1). But, as seen in Fig. 3, increasing the time delay resulted in another sequence: no propagation, a continuous circular wavefront, spiral and, again, a circular wavefront. Responses to excitation within the VR associated with class 3 of wavefronts were observed to evolve into two different patterns: a circular wave and a pair of spiral waves. The underlying mechanism is the well known effect of merging and annihilation of rotating waves when they are spaced too close one to another.

The different evolution of the broken waves

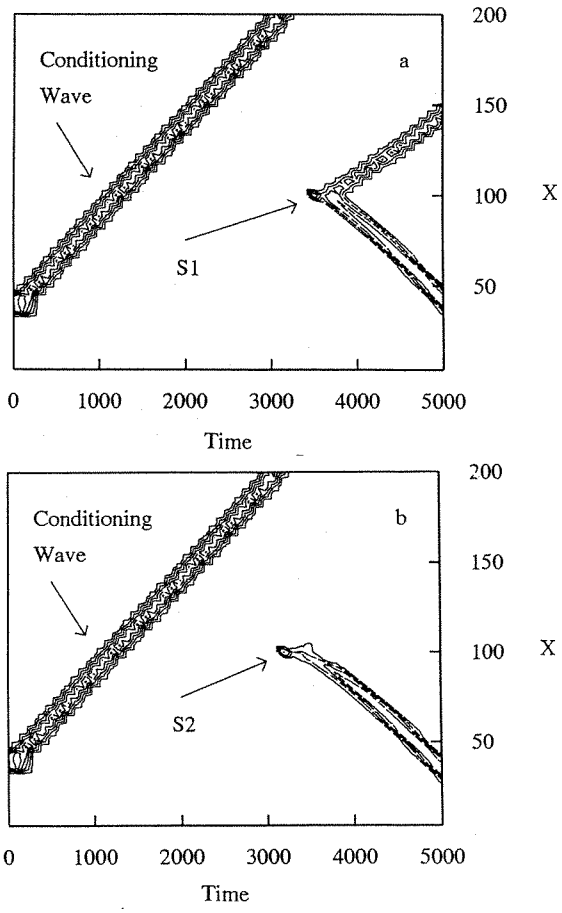

Fig. 2. Analog of vulnerability in 1D. Two stimuli were delivered in a way similar to the ones shown in Fig. 1. The time delay between the conditioning wave and the stimulus, s, was 2.361 time units (t.u.) in (a), and 1.861 t.u. in (b). The stimulus $s1$ in (a) propagated in both directions (corresponding to a circular wave in 2D), while the stimulus $s2$ in (b) propagated unidirectionally (corresponding to a broken wavefront in 2D, which can generate a pair of spirals in the VR). A projection of the u variable behaviour is shown (Oregonator model parameters $f = 3.0$, $\varepsilon = 0.05$, $q = 0.002$).

was related to the spatial size of the test perturbation. This size was numerically modified (Fig. 3), both in the direction parallel to the movement of the conditioning wavefront (P_x) and in the perpendicular one (P_y).

The region of vulnerability increased when the size of the perturbation was increased. The quantitative behaviour was different for X and Y directions (Fig. 3). The increase of the spatial size (P_y) of the perturbed region increased the

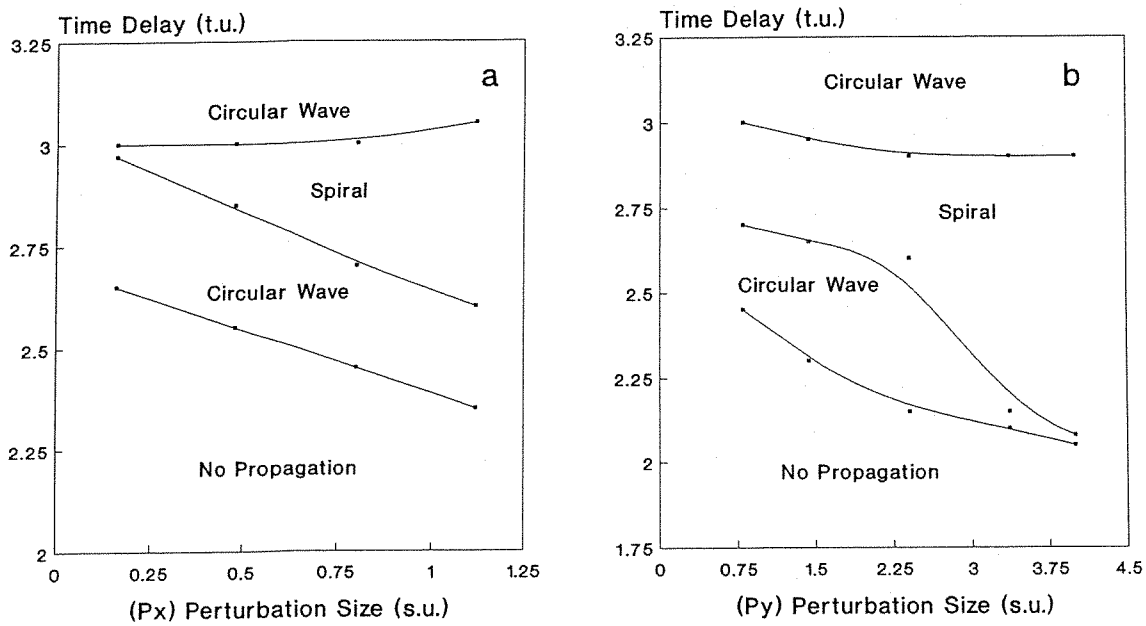

Fig. 3. Effect of the size of the stimulated region on the vulnerability in 2D (numerically simulated in the Oregonator model). (a) The dependence on the size of the perturbation in the X direction, P_x (perpendicular to the conditioning wavefront). The region of vulnerability (spiral formation) increases when P_x is increased (P_y was kept constant, $P_y = 0.80$ spatial units (s.u.)). (b) The dependence on the size of the perturbation in the Y direction, P_y (parallel to the conditioning wavefront). The region of vulnerability also increases when P_y is increased. The increase is not regular: for small and big values of P_y, small changes almost do not affect the region of vulnerability. For intermediate values of P_y (between 2.4 and 3.0 s.u.), small changes in its value produce significant changes in the region of vulnerability (P_x was kept constant, $P_x = 0.80$ s.u.) (Oregonator model parameters $f = 3.0$, $\varepsilon = 0.06$ and $q = 0.002$).

distance between the two wavebreaks. This perturbation separated the two initiating spirals by enough distance such that they could evolve without annihilation. The increase of the spatial size (P_x) of the perturbed region increased the probability of having a part of the perturbation within the VR.

In Fig. 4, we plot the evolution of responses for different perturbation geometries. Increasing the perturbation size in any direction resulted in spiral wave formation (for a small size of the perturbation, only circular waves were observed).

Dependence of VR on the excitability of the medium is shown in Figs. 5 and 6. The region of vulnerability decreases as the excitability of the medium is increased. The two regions of circular waves were observed in the 2D case both experimentally and numerically (Figs. 5 and 6b).

5. Discussion

Disturbing the BZ reaction has often been used to initiate spiral waves. The nature of the disturbance and the resultant response, however, has received little attention. While this question has been overlooked in studies of chemical reactions, the question has received considerable attention within the cardiology community [6,9,10,12,13] – primarily because the initiation of a spiral pattern of excitation in the heart can lead to disturbances in cardiac rhythm that result in *sudden cardiac death*.

To establish a frame of reference, we have defined vulnerability as the ability to establish a discontinuous wavefront – i.e. a wavefront that propagates in some directions and fails to propagate in other directions relative to a stimulation site.

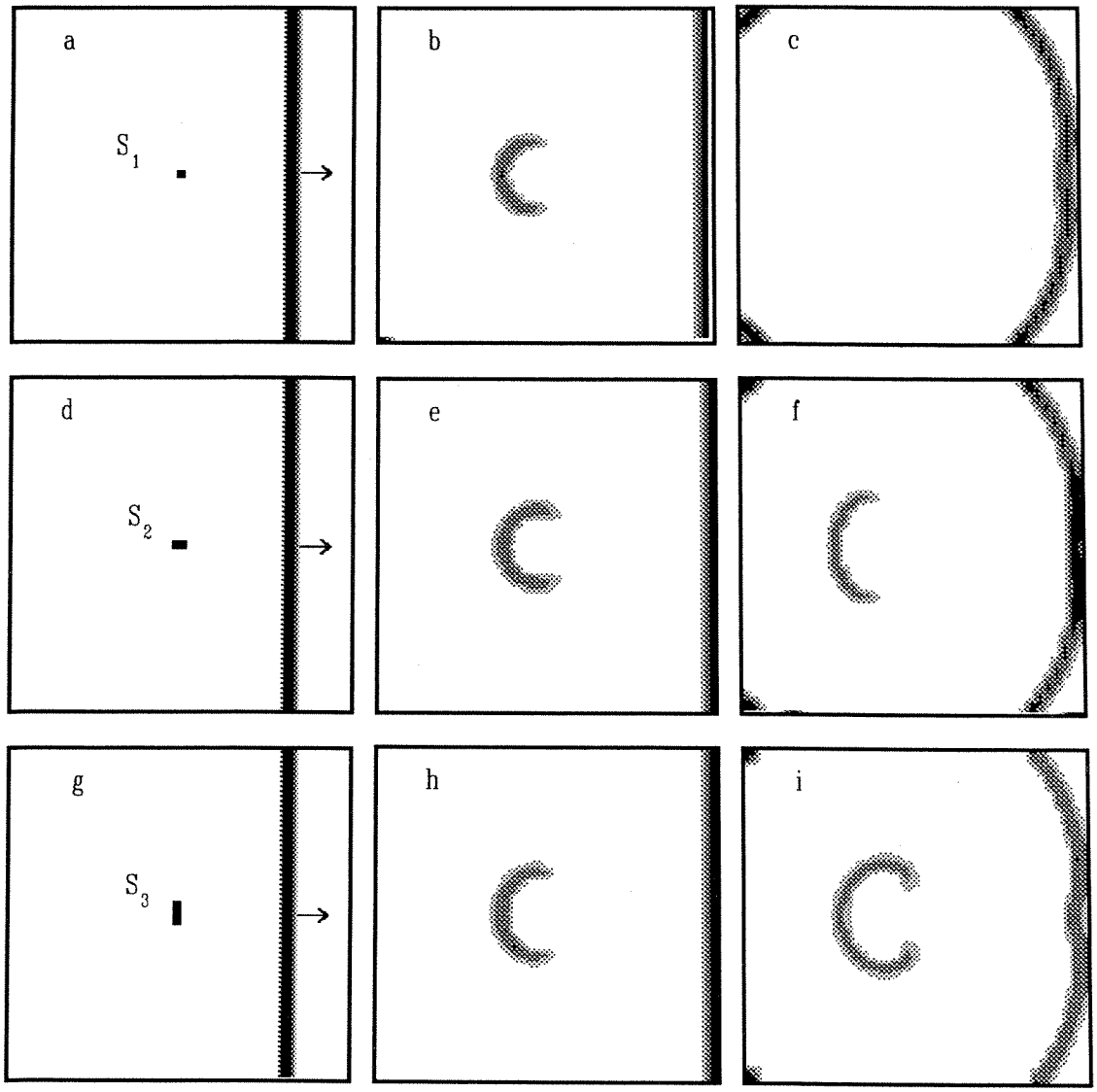

Fig. 4. Evolution of wave patterns for different sizes of the stimulated region (numerically simulated in the Oregonator model). In panels (a) to (c), the evolution for a squared perturbation, $s1$, ($s1 = (P_{x1} = 0.80,\ P_{y1} = 0.80)$ s.u.) is shown, for instants $t = 0$, $t = 2.5$ and $t = 5.0$ t.u. The result is a circular wave. In panels (d) of (f), the evolution for a rectangular perturbation, $s2$, oriented in the X direction, ($s2 = (P_{x2} = 1.44,\ P_{y2} = 0.80)$ s.u.), for the same instants, is shown. The result is a discontinuous wavefront that evolves in a pair of spiral waves. In panels (g) to (i), the evolution for a rectangular perturbation, $s3$, oriented in the Y direction ($s3 = (P_{x3} = 0.80,\ P_{y3} = 2.40)$ s.u.), for the same instants, is shown. The result is a discontinuous wavefront that evolves in a pair of spiral waves. (Oregonator model parameters $f = 3.0$, $\varepsilon = 0.06$ and $q = 0.002$).

Our results extend observations in Spach's experiments on vulnerability in cardiac muscle and Keener's theoretical analysis. We have shown that the phenomenon of vulnerability is not exclusive for discrete systems, and the existence of propagation failure in discrete systems is not a general explanation. We have found that the mechanism responsible is the generic be-

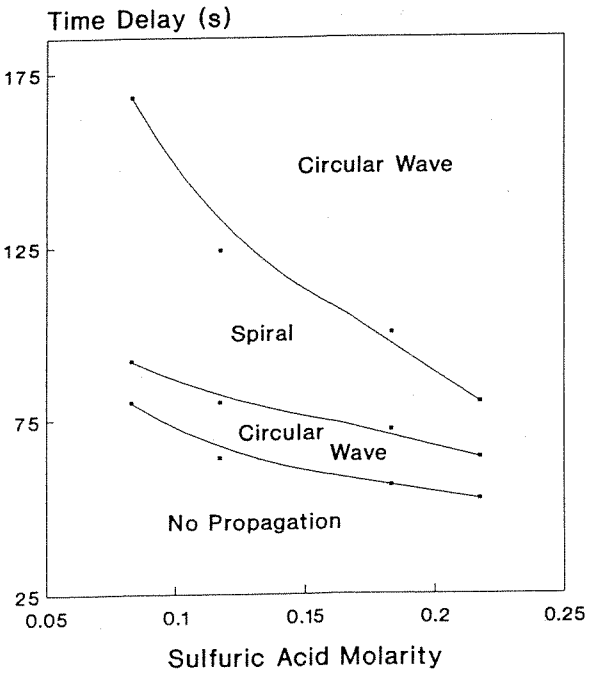

Fig. 5. Excitability effect on vulnerability (in BZ experiment). Time delay is plotted versus the excitability of the medium, which is proportional to the sulfuric acid concentration. The vulnerability region (spiral formation) decreases when the excitability of the system is increased.

haviour of excitable systems, and rotating spiral waves can be obtained in a continuous system with isotropic diffusion coefficients (this is the case in BZ, but not in cardiac muscle).

It was earlier suggested [18] that vulnerability can be observed in the BZ reagent. A liquid-phase reaction was used in this experiment, which is inevitably heterogeneous: due to the inhibitory effect of oxygen, the excitability increases with depth of the medium. To overcome this difficulty, catalyst immobilized in a gel was used in our experiments. In this case, the medium is homogeneous (no changes of excitability with the depth), and at the same time, convention effects due to the silver wire introduction into the liquid layer were avoided. In addition, it permitted us to obtain a *quasi* bidimensional contact between the gel and the silver wire used to deliver the stimuli.

We found that disturbing the BZ reaction

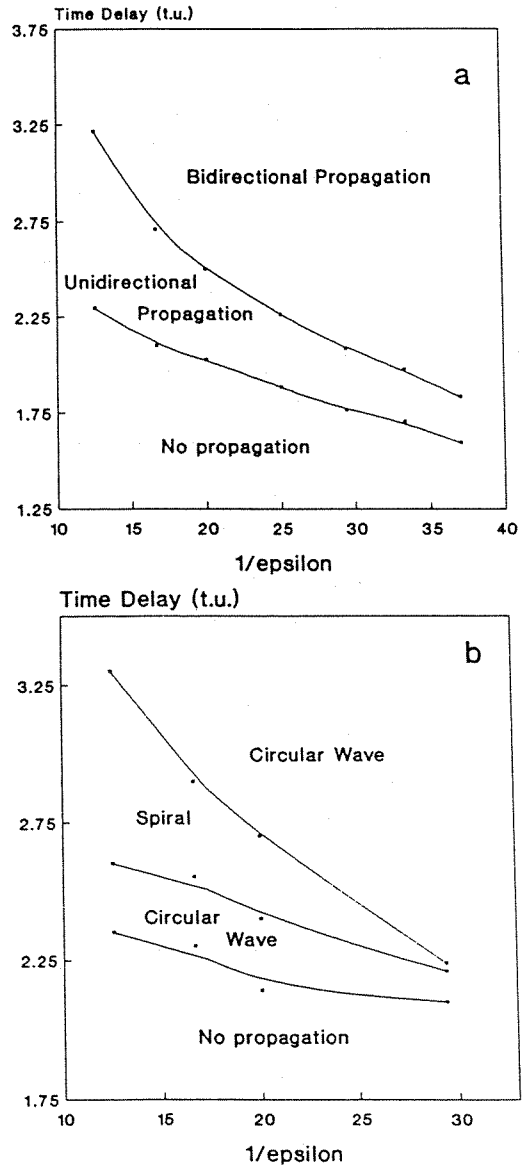

Fig. 6. Excitability effect on the vulnerability (numerically simulated in the Oregonator model). Time delay is plotted versus the excitability of the medium, which is proportional to $1/\varepsilon$ in the model. (a) 1D. The vulnerability region (unidirectional propagation) decreases when the excitability of the system is increased. (b) 2D. The vulnerability region (spirals formation) also decreases when the excitability of the system is increased. Note that the increase of the dimensionality results in the diminishing of the diminishing of the VR and the qualitative agreement between Figs. 6b and 5 obtained numerically and experimentally. The size of the perturbation both in X and in Y directions was $P_x = P_y = 0.80$ s.u. and the parameters in the Oregonator model $f = 3.0$ and $q = 0.002$.

produced either continuous or discontinuous (broken) waves. The discontinuous fronts eventually evolved into either a pair of spirals (at the points of discontinuity) or, if the distance between points of discontinuity was too small, wavefront continuity was re-established and a circular wave resulted. This is related to the fact that, when the free ends (*tips*) of two spirals are situated too close, they collide and annihilate giving rise to a continuous wavefront. Thus, a critical distance between the free ends of a broken front is required to evolve into a pair of spirals, and this distance is increased with the perturbation size.

The difference in the evolutionary patterns associated with the discontinuous wavefront was related to the size of the stimulus perturbation relative to the direction of propagation of the conditioning wavefront. Increasing the size of the perturbation in the direction parallel to the conditioning wave, P_y, resulted in an increase of the VR because this perturbation increased the distance between the two wavebreaks. In this case, the two free ends of a broken wave evolved into a pair of spirals (while with a smaller size P_y of the perturbation, they evolved into a continuous wave 3b). Note (Fig. 3b) that the increase of the VR is not monotonic in P_y. Thus, for small and big values of P_y, small changes affect slightly the VR, while for intermediate values small changes have a significant effect on the VR size. This is due to the existence of a critical distance between spiral tips which avoids their collision and annihilation. For values of P_y close to the distance, small changes in P_y affect strongly the VR size.

Increasing the size of the perturbation in the direction perpendicular to the conditioning wavefront, P_x, resulted in an increase of the VR. That is because even if the perturbed region was situated outside the vulnerability region, say at the distance L from it, then changing $P_x \rightarrow P_x + L$ will guarantee that the perturbation will at least touch the VR. This effect exists both in 1D and 2D media.

Our results, obtained with the BZ experiment and with the Oregonator model, are qualitatively in agreement with the dependence of the lifetime of a pair of rotating vortices on the initial distance between them, measured by Panfilov and Vasiev [22] with the FitzHugh–Nagumo model.

Throughout our experiments, the evolution of an initially discontinuous wavefront can be understood in terms of the dimensionality of the medium. In 2D, a broken wave curls up to give a rotating spiral wave, as we have mentioned before. In 1D, a perturbation delivered with the same delay (class 3 responses) will result in only one propagating pulse. If this 1D experiment would be performed with an excitable fiber closed to a circle (periodical boundary conditions), this would give rise to a rotating pulse.

For 1D excitable systems, there is an approximated relation between the VR, length l of the perturbed region, and the propagation velocity [23,24] ϕ:

$$l/\phi > \mathrm{VR}\,. \tag{2}$$

From this relationship, we see that an increase of excitability which increases the wavefront propagation velocity also diminishes the VR (Figs. 5,6).

Acknowledgments

This work was supported in part by the "Comisión Interministerial de Ciencia y Tecnología" (Spain) under project DGICYT-PB91-0660.

References

[1] D. Barkley, Phys., Rev. A 42 (1990) 2489–2492.
[2] A.S. Mikhailov and V.S. Zykov, Physica D 52 (1991) 379–397.
[3] A.T. Winfree, in: The Geometry of Biological Time (Springer, Berlin, 1980).
[4] A.T. Winfree, Physica D 49 (1991) 125–140.

[5] V.S. Zykov, Biophysics 31 (1986) 940–944.
[6] M.A. Allessie, F.I.M. Bonke and T.Y.G. Scopman, Circ. Res. 33 (1973) 54–62.
[7] N.A. Goroleva and J. Bures, J. Neurobiol. 14 (1983) 353–363.
[8] A. Robertson and A.F. Grutsch, Cell 24 (1983) 603–611.
[9] M.S. Spach, W.T. Miller, D.B. Geselowitz, R.C. Borr, J.M. Kootsey and E.A. Johnson, Circ. Res. 48 (1981) 39–54.
[10] F.J.L. Van Capelle, Slow Conduction and Cardiac Arrhythmias, Thesis, University of Amsterdam (1983).
[11] A.T. Winfree, Scientific American 248 (1983) 144–161.
[12] C.F. Starmer, A.A. Lastra, V.V. Nesterenko and A.O. Grant, Circulation 84 (1991) 1364–1367.
[13] J.P. Keener and F.M. Phelps, in: Lectures on Mathematics in Life Sciences, Vol. 21 (American Mathematical Society 1989) pp. 151–181.
[14] A.M. Zhabotinsky and A.N. Zaiken, in: Oscillatory Processes in Biological and Chemical Systems, Vol. 2 (1971).
[15] T. Yamaguchi, L. Kunhert, Z. Nagy-Unguaray, S.C. Müller and B. Hess, J. Phys. Chem. 95 (1991) 5831–5837.
[16] G.S. Skinner and H.L. Swinney, Physica D 48 (1991) 1–16.
[17] V. Pérez-Muñuzuri, R. Aliev, B. Vasiev and V.I. Krinsky, Physica D 56 (1992) 229–234.
[18] C.F. Starmer, V.I. Krinsky, D.S. Romashko, R.R. Aliev and M.R. Stepanov, in: Spatio-temporal Organization in Nonequilibrium Systems, ed. S.C. Múller and T. Plesser (Projekt Verlag, 1992) pp. 254–256.
[19] M. Gómez-Gesteira, G. Fernández-García, A.P. Muñuzuri, V. Pérez-Muñuzuri, V.I. Krinsky, C.F. Starmer and V. Pérez-Villar, Int. J. Bif. Chaos 4(5) (1994), to appear.
[20] R.J. Field, E. Koros and R.M. Noyes, J. Am. Chem. Soc. 94 (1972) 8649.
[21] J.P. Keener and J.J. Tyson, Physica D 21 (1986) 307–324.
[22] A.V. Panfilov and B.N. Vasiev, Physica D 49 (1991) 107–113.
[23] A.P. Muñuzuri, M. Gómez-Gesteira, V. Pérez-Muñuzuri, V.I. Krinsky and V. Pérez-Villar, Phys. Rev. E 48 (1993) 3232–3235.
[24] C.F. Starmer, D.N. Romashcko, V. Bitkashev, M. Stepanov, O.N. Makarova and V.I. Krinsky, Biophys. J. 65 (1993) 1775–1787.